The Astrophysical Journal Letters, 733:L29 (6pp), 2011 June 1 doi:10.1088/2041-8205/733/2/L29

A SEARCH FOR CONCENTRIC CIRCLES IN THE 7 YEAR *WILKINSON MICROWAVE ANISOTROPY PROBE* TEMPERATURE SKY MAPS

I. K. Wehus[1,2] and H. K. Eriksen[3,4]
[1] Department of Physics, University of Oslo, P.O. Box 1048 Blindern, N-0316 Oslo, Norway; i.k.wehus@fys.uio.no
[2] Theoretical Physics, Imperial College London, London SW7 2AZ, UK
[3] Institute of Theoretical Astrophysics, University of Oslo, P.O. Box 1029 Blindern, N-0315 Oslo, Norway
[4] Centre of Mathematics for Applications, University of Oslo, P.O. Box 1053 Blindern, N-0316 Oslo, Norway
Received 2010 December 6; accepted 2011 April 13; published 2011 May 9

ABSTRACT

In this Letter, we search for concentric circles with low variance in cosmic microwave background sky maps. The detection of such circles would hint at new physics beyond the current cosmological concordance model, which states that the universe is isotropic and homogeneous, and filled with Gaussian fluctuations. We first describe a set of methods designed to detect such circles, based on matched filters and χ^2 statistics, and then apply these methods to the best current publicly available data, the 7 year *Wilkinson Microwave Anisotropy Probe* (*WMAP*) temperature sky maps. We compare the observations with an ensemble of 1000 Gaussian ΛCDM simulations. Based on these tests, we conclude that the *WMAP* sky maps are fully compatible with the Gaussian and isotropic hypothesis as measured by low-variance ring statistics.

Key words: cosmic background radiation – cosmology: observations – methods: statistical

Online-only material: color figure

1. INTRODUCTION

One of the main accomplishments in cosmology during the last decade is the establishment of the ΛCDM inflationary concordance model. According to this model, the universe consists of 5% baryonic matter, 22% dark matter, and 73% dark energy (Jarosik et al. 2011), and is filled with random and Gaussian fluctuations. These fluctuations were generated during a short period of exponential expansion called inflation (e.g., Liddle & Lyth 2000, and references therein), during which the universe expanded by a factor of $\sim 10^{26}$ in $\sim 10^{-34}$ s. With only a handful of free parameters, this model is able to successfully fit thousands of observational data points.

Nevertheless, the ΛCDM model must at the current stage be considered an effective model rather than a fundamental model. First, it relies on several quantities that have never been directly observed except through their gravitational impact, such as both dark matter and dark energy. Second, it postulates the existence of an unknown scalar field, the inflaton. It is therefore important to put the inflationary framework to stringent tests, probing its range of validity in different ways. One approach to do so is to construct alternative cosmological theories, making different observational predictions than ΛCDM, and then compare the two models using high-precision data.

One common approach to this problem is to search for features not predicted by the isotropic and homogeneous model. A few examples extensively discussed in the literature include local non-Gaussianity, large-scale correlations, coherent spots, and hemispherical power asymmetries (e.g., Bennett et al. 2011, and references therein). Other authors search for coherent circles of various forms in the cosmic microwave background (CMB) field, which in some theories might represent a specific signature of new physics.

A well-established form of coherent circles in the CMB field is that due to closed topologies (Cornish et al. 1998). If the universe has a closed topology, and a radius not much greater than the horizon, we should expect to see the same CMB pattern in two different directions on the sky in the form of two *matched circles*. Many searches for such signatures have been performed, the most recent by Bielewicz & Banday (2011), but so far all have resulted in negative results.

A second example of CMB rings is provided by models of pre-inflationary massive particles (Fialkov et al. 2010). These predict the existence of concentric hot and cold rings in the CMB, as well as a bulk flow of galaxies toward their center. Kovetz et al. (2010) have analyzed the *WMAP* data and claim to find evidence statistically significant at the 3σ confidence level.

A third example is presented by Feeney et al. (2010), searching for evidence of the multiverse in the form of bubble collisions leaving circular patterns in our CMB sky. Also this group compares *WMAP* data with simulations and claim to find hints of evidence for their model in the *WMAP* sky maps.

A fourth recent example is that of Gurzadyan & Penrose (2010), who start from the cyclic cosmology presented by Penrose (2008, 2009, 2010). They claim that in this picture, collisions of massive black holes would result in a set of concentric circles of low variance in the CMB field. They also claim to see tentative evidence for such features, in the form of positions with possibly anomalous variance profiles.

In this Letter, we perform a proper statistical search for such concentric low-variance circles in the *WMAP* temperature maps. The results are model independent and should be useful to any theorist working on models that predict such rings. We also note that a conceptually similar analysis was publicly presented by Moss et al. (2010) on the same day as the present Letter, reaching fully consistent results.

2. DATA AND SIMULATIONS

The main goal of this Letter is to search for coherent circles of low variance centered on a central position, $\hat{p}$, in the CMB anisotropy field, $\Delta T(\hat{n})$, observed today. In this

Letter, we therefore consider the best currently available full-sky maps of the CMB, namely the 7 year *WMAP* temperature sky maps. These data are provided at Lambda[5] in the form of pixelized HEALPix sky maps with a pixel resolution of 7′.

In this Letter we consider the foreground-reduced *WMAP* *W*-band (94 GHz) data, which has the highest resolution of all the *WMAP* bands, corresponding to an angular resolution of 13′ FWHM. We apply the *WMAP* KQ85 sky cut to this map, removing 22% of the sky, and take into account both the galactic plane and high-latitude point sources (Gold et al. 2011).

Next, we build an ensemble of 1000 simulations with a spectrum given by the best-fit *WMAP* 7 year ΛCDM model (Komatsu et al. 2011). These realizations are convolved with the *W*-band beam and HEALPix pixel window, and projected onto a HEALPix $N_{\mathrm{side}} = 512$ grid. Finally, uncorrelated inhomogeneous Gaussian noise with RMS equal to $\sigma_0/\sqrt{N_{\mathrm{obs}}(p)}$ are added to pixel p, where σ_0 is the *W*-band noise RMS per observation and $N_{\mathrm{obs}}(p)$ is the number of observations in that pixel. The KQ85 sky cut is also applied to the simulations.

We also consider one end-to-end 7 year *WMAP W*-band simulation, as provided by the *WMAP* team. This simulation takes into account all known systematic effects, including correlated noise and correlations between radiometers, thermal drifts, sampling effects, sidelobe pickup, etc. Because only one such simulation has been made available by the *WMAP* team, it is not possible to make a complete comparison between the real *WMAP* data and an ensemble of such simulations. Fortunately, this also turns out to be unnecessary: using our main statistic, we find that the *WMAP* data are fully compatible with the basic CMB plus white noise model, as is the end-to-end simulation. This indicates that any possible instrumental effects are strongly subdominant to the CMB cosmic variance and instrumental white noise. Of course, this conclusion is not unexpected, given the excellent performance of the *WMAP* satellite (e.g., Jarosik et al. 2011).

3. METHOD

A central concept in the following search is the radial standard deviation profile,[6]

$$\sigma_p(b) \equiv \sqrt{\frac{1}{N-1}\sum_{\theta\in b}\Delta T(n)^2}, \tag{1}$$

where p denotes a fixed reference pixel on the sky, n is a variable pixel index, and $\theta = \mathrm{acos}(\hat{p}\cdot\hat{n})$ is the angular distance between those two positions; b denotes an angular bin, $[\theta_{b-1}, \theta_b)$. Thus, this function measures the standard deviation of the CMB field as a function of radial distance from p, and a sharp negative spike in this function corresponds to the postulated signature of the black hole collisions. To reduce correlations between different bins, we subtract the mean from each function $\sigma_p(b)$ separately before further processing.

We measure $\sigma_p(b)$ for all positions over a HEALPix $N_{\mathrm{side}} = 32$ grid, for a total of 12,288 points. Each function is evaluated from 0 to 20° in 40 bins, corresponding to a bin size of 0°.5. If more than 40% of the pixels within 20° of a given pixel p are masked out, that pixel is removed from further analysis. Finally, we also remove any pixels that are immediate neighbors to the galactic cut.

Having computed these functions for both data and simulations, the next step is to identify potential low-variance ring candidates and quantify their significance. To this end, we introduce two different statistics. First, we consider matched filters designed to highlight negative spikes in $\sigma_p(b)$,

$$\hat{\sigma}_p(b) = \sum_{b'}\sigma_p(b')f(b'-b). \tag{2}$$

Here $f(b)$ defines a discrete filter, and we consider three different cases in this Letter, namely, $f_1 = [0.5, -1, 0.5]$, $f_2 = [0.25, 0.25, -0.5, -0.5, 0.25, 0.25]$, and $f_3 = [0.5, -0.125, -0.75, -0.125, 0.5]$; for $|b-b'|$ larger than the length of the filter, f is zero. These filters correspond to (1) a negative top-hat filter of width 1, (2) a negative top-hat filter of width 2, and (3) a negative wedge filter, each sensitive to typical interesting candidates. For each case, we adopt the maximum of $\hat{\sigma}_p(b)$ as our statistic, considering only angular distances larger than 2° as the intrinsic estimator variance is very large on the smallest scales. We then make both sky maps and histograms of the maximum values of $\hat{\sigma}_p(b)$ and compare these between the observed data and the simulations.

Our second statistic is based on the standard χ^2 estimator, which is sensitive to the overall fluctuation level of $\sigma_p(b)$, rather than individual spikes. Specifically, we compute

$$\chi^2 = \sum_{bb'}(\sigma_p(b)-\mu_b)C^{-1}_{bb'}(\sigma_p(b')-\mu_{b'}) \tag{3}$$

for each pixel and data set, where μ_b is the mean of $\sigma_p(b)$ computed from the simulation set and $C_{bb'}$ is the covariance matrix. Again, we make sky maps of these values for the observed data and compare the observed data with the simulations in terms of histograms.

We finally define a test that explicitly searches for points with multiple strong low-variance rings: a consecutive set of bins is defined to form a low-variance ring if (1) the standard deviation profile drops by more than 12 μK at the beginning of the ring and then increases by more than 12 μK at the end of the ring, and (2) the total width of the ring is not more than 1°.5, i.e., corresponding to a width of 3 angular bins. We then locate the pixel with the highest number of such rings and plot the corresponding variance profile.

4. RESULTS

We now present the results obtained from the analysis outlined above as applied to the 7 year *WMAP* data. First, the left panel of Figure 1 shows the standard deviation profile computed from the *WMAP* data centered on Galactic coordinates $(l, b) = (105°.04, 37°)$. (The mean is not subtracted in this plot.) This is the same profile as that presented in Figure 2 of Gurzadyan & Penrose (2010) and mentioned as a possible statistical anomaly. As seen here, we obtain very similar results as Gurzadyan & Penrose (2010), and this validates the computational routines used in both analyses. The right panel shows a corresponding profile computed from a random simulation.

In the same figures, we also plot the mean of the variance profiles computed from all pixels, together with the corresponding 1σ and 2σ confidence regions. Here we note several interesting features. First, the *WMAP* example profile is consistently low compared with the mean, suggesting strong correlations

[5] http://lambda.gsfc.nasa.gov

[6] We use the terms "standard deviation profile" and "variance profile" interchangeably in this Letter.

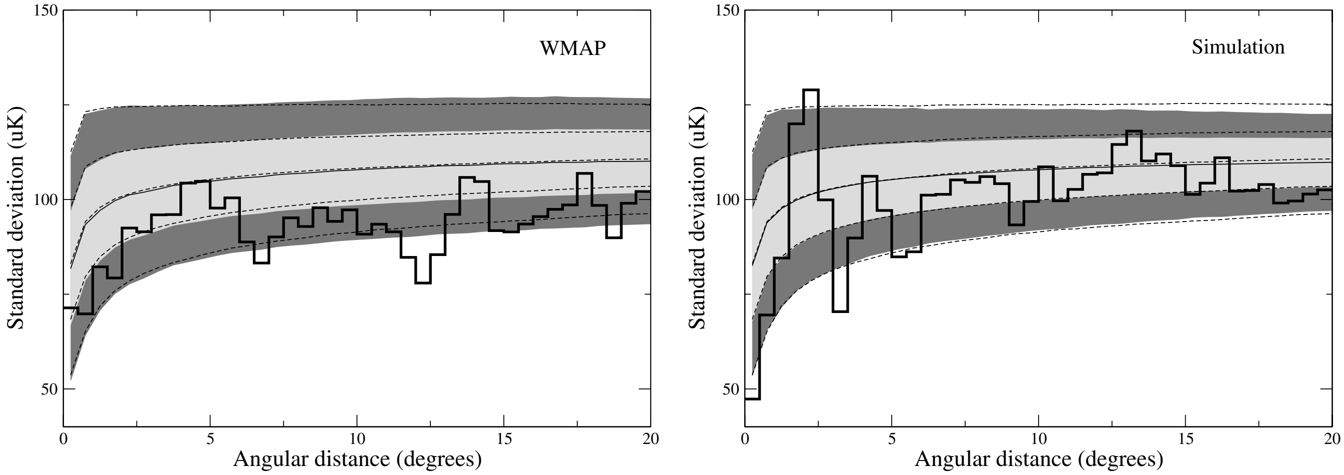

Figure 1. Examples of single standard deviation profiles (thick histograms), computed from *WMAP* (left) and a simulation (right). The thin solid line shows the mean of all profiles and the shaded regions show the 1σ and 2σ confidence regions. The dashed curves indicate the mean and 1σ and 2σ confidence regions computed from the end-to-end simulation; the slight variations between the various confidence regions are fully compatible with variations seen between different white noise simulations. The *WMAP* profile is centered on galactic coordinates $(l, b) = (105^\circ\!.04, 37^\circ)$, reproducing Figure 2 of Gurzadyan & Penrose (2010). Note that low-variance rings are found also in the simulation.

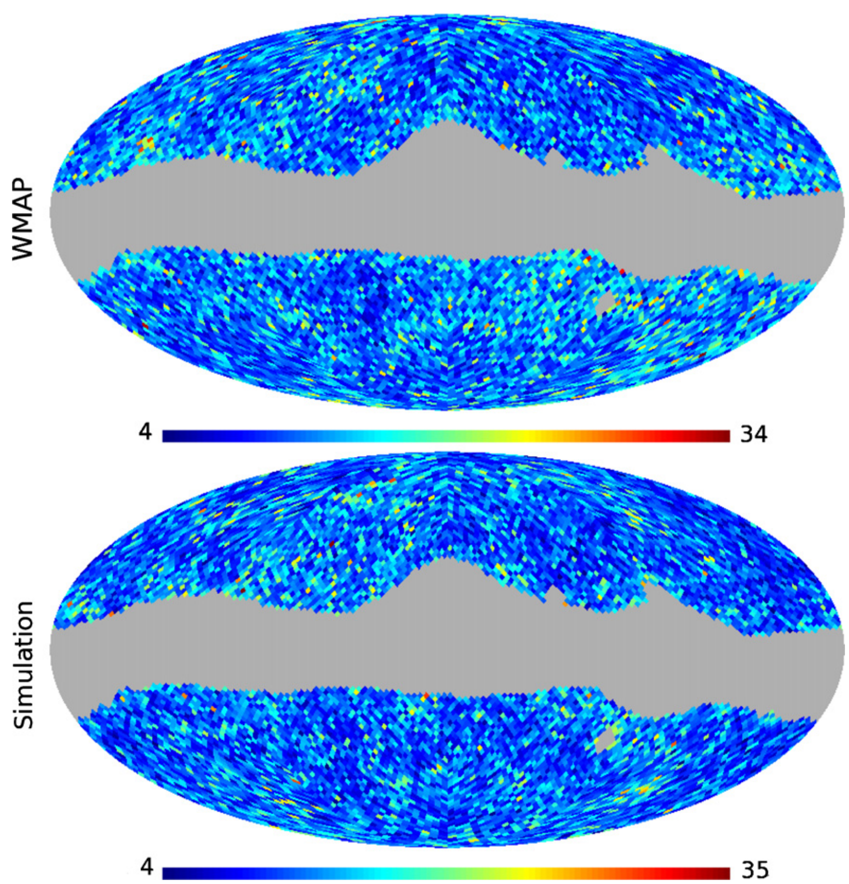

Figure 2. Example of sky maps obtained by the matched filter searches, in this case the wedge filter, f_3. The top panel shows the map obtained from *WMAP*, the bottom panel shows the same for a random simulation.

(A color version of this figure is available in the online journal.)

between bins. This is typical for all profiles for both *WMAP* and simulations; the local variance in a CMB map depends on the scanning strategy of *WMAP*, and the entire profile can shift up or down depending on whether the corresponding pixel is located in the ecliptic plane (high noise) or in the ecliptic poles (low noise). Since this effect is of little interest in the search for concentric rings, we subtract the mean before further analysis to reduce bin-to-bin correlations.

Next, we note that the simulated distribution is very similar to that of *WMAP*, having consistent mean and standard deviation. We have also checked that this distribution is consistent from simulation to simulation.

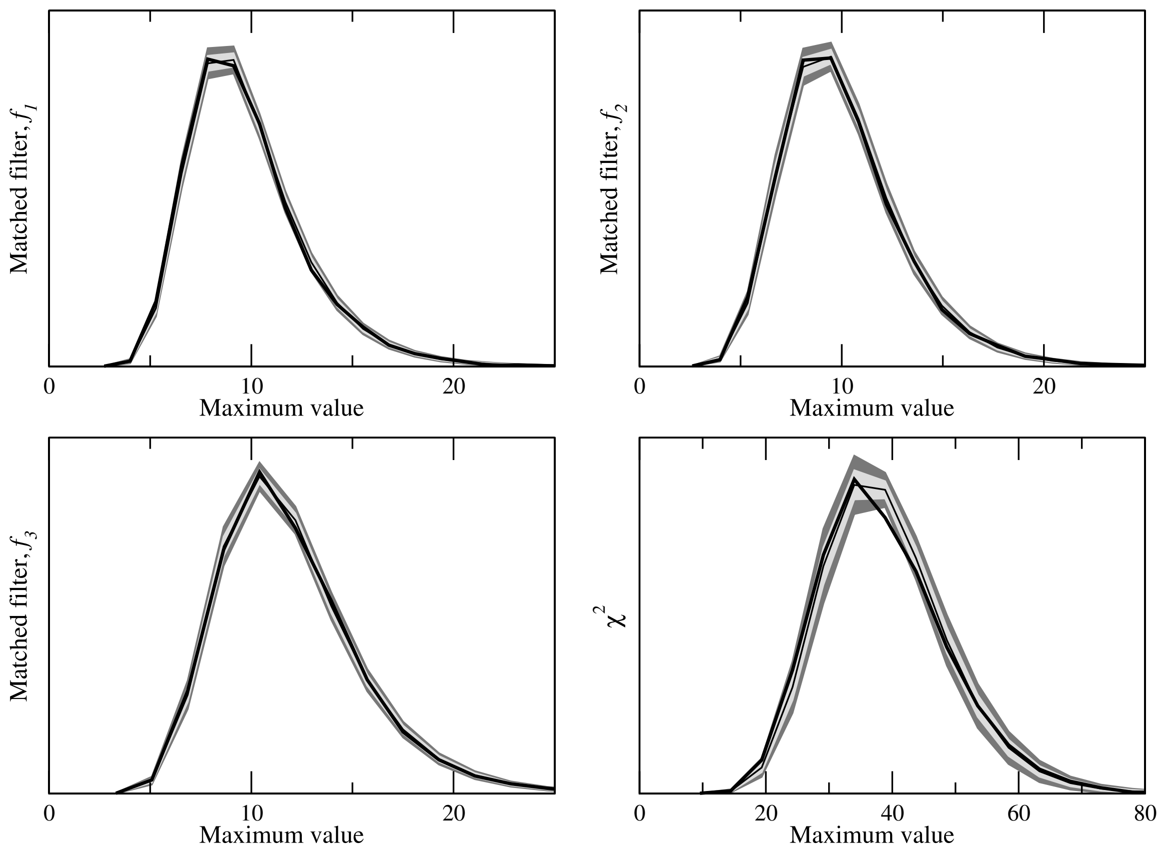

Figure 3. Histogram comparison between the *WMAP* data (thick solid lines) and the ΛCDM simulations (mean in thin black lines; 1σ and 2σ regions in gray bands), for each of the four statistics adopted in this Letter.

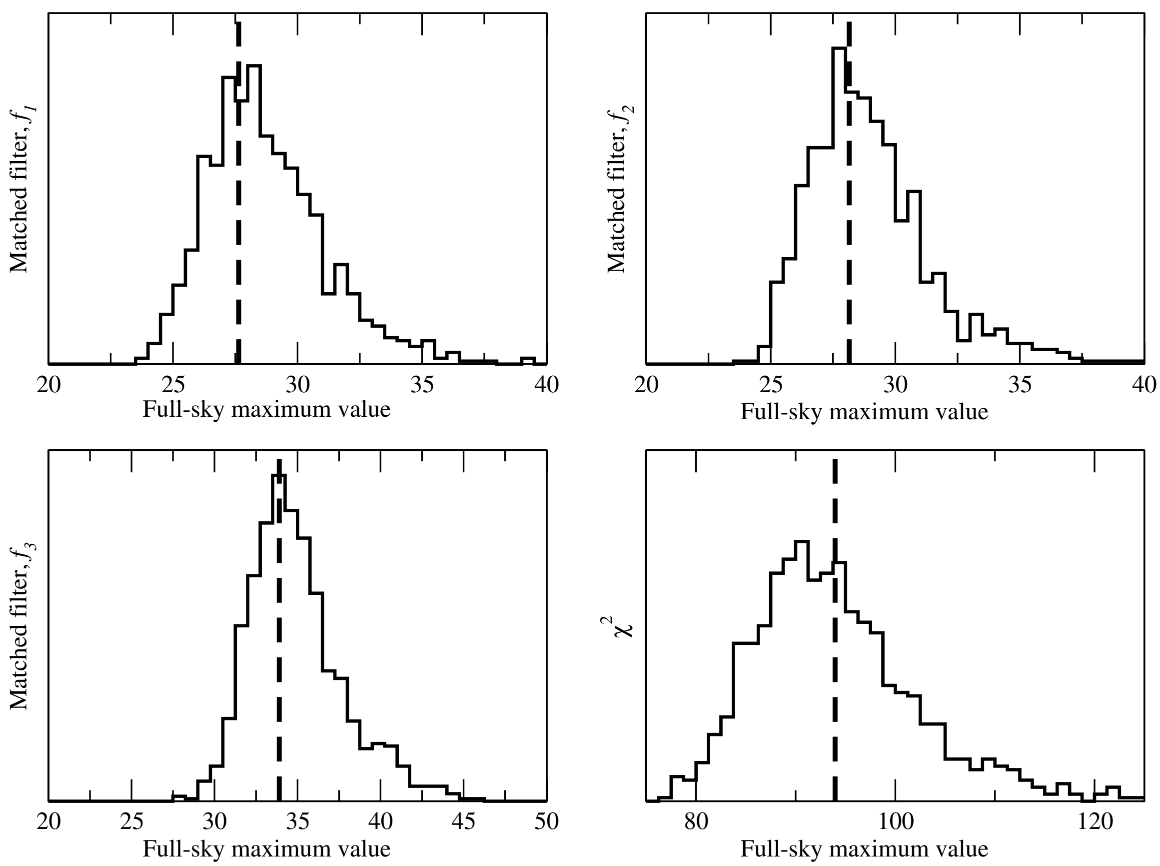

Figure 4. Comparison of the full-sky maximum value for each statistic between the simulations (histograms) and the *WMAP* data (vertical dashed line).

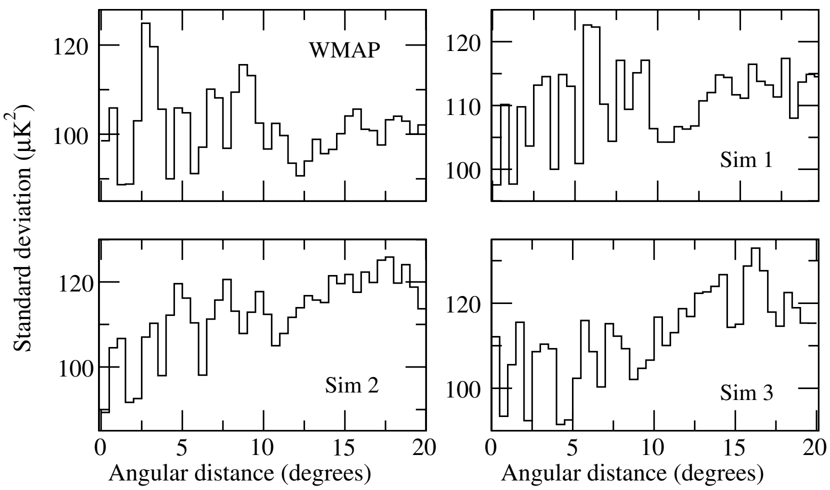

Figure 5. Variance profiles computed from both the *WMAP* data (top left panel) and three simulations showing multiple concentric circles.

Returning to the left panel of Figure 1, the most extreme outlier in the *WMAP* example has a value of 77 μK at an angular distance of 12°.5. At the same distance the expected value is 109 ± 10 μK, and this outlier thus corresponds to a $\sim 3.2\sigma$ outlier. From this purely visual impression, one might therefore wonder whether this point might be anomalous compared with the standard ΛCDM model. However, as seen in the right panel of Figure 1, we see that even the simulated data set exhibits similar outliers.

To address these issues more rigorously, we are therefore led to adopt proper statistical techniques; visual inspection is not sufficient. To this end, we employ the search algorithms described in Section 3 to identify peculiar candidates in both the data and simulations, and consider various statistics based on these results to interpret significances statistically.

In Figure 2, we show sky maps of the third matched filter, f_3, statistic, where each pixel indicates the maximum of $\hat{\sigma}_p(b)$ over b. Thus, pixels with large values in these plots indicate variance profiles with a notable negative wedge-like structure. Such maps are shown for both the *WMAP* data and a random simulation. At least visually, the two maps appear statistically consistent.

This statement is quantified more rigorously in Figure 3, where we show histograms for each of the four statistics computed from the *WMAP* data, and compared to the mean properties of the simulated ensemble. Again, the *WMAP* properties appear fully consistent with the simulations.

However, the histogram statistics shown above are sensitive only to the mean properties of the CMB field. They only show that there is no evidence for a large number of concentric circles in the *WMAP* data, not that there cannot be a small number of highly significant cases. We therefore also consider the maximum value of each of the four statistics, which should be sensitive to single extreme cases. Figure 4 shows histograms of such maximum values, as computed from the simulated ensemble, with the corresponding *WMAP* value indicated by a vertical line. Again, we see that *WMAP* appears fully consistent with the ΛCDM simulations.

Finally, Figure 5 shows the variance profiles with the highest number of individual >12 μK rings, as defined in the last paragraph of Section 3. For *WMAP* we can see four such low-variance rings, while for the three simulations shown here (which were simulations 1–3 in our full simulation set), there are four, three, and four rings, respectively. Also for this test, *WMAP* appears fully consistent with the ΛCDM simulations.

5. CONCLUDING REMARKS

In this Letter, we search for concentric low-variance rings in the 7 year *WMAP* temperature sky maps. This work adds to an already extensive literature on non-standard CMB signatures, seeking to challenge the current cosmological concordance model, which assumes that the universe is isotropic and homogeneous, and filled with Gaussian fluctuations. Potential detections of concentric low-variance rings would suggest new physics, similar to how the presence matched circles in the CMB field might imply the reality of non-trivial topologies.

We have defined three different statistical tests suitable to locate and quantify such rings, based on matched filters, χ^2 statistics and thresholding. We then applied these methods both to the actual *WMAP* temperature sky map and to a simulated ensemble of 1000 realizations drawn from a standard ΛCDM power spectrum.

The results from our search are negative: as far as our current statistics are concerned, the *WMAP* data appear fully compatible with the ΛCDM model. Both the number and magnitude of any degree-scale low-variance rings in the *WMAP* data are explained in terms of cosmic variance in the *WMAP* data. Of course, this does not exclude the existence of other anomalous rings in the *WMAP* data, be that either thinner (or smaller) rings, rings of coherent temperature values or even matched circles, and so the search for anomalous features will certainly go on. However, unless a clear tentative detection of low-variance circles from real data is presented, or possibly a robust theoretical prediction based on a sound physical model, this particular form of CMB anomaly does not appear to be the most promising for further study.

The computations presented in this Letter were carried out on Titan, a cluster owned and maintained by the University of Oslo and NOTUR. Some of the results in this Letter have been derived using the HEALPix (Górski et al. 2005) software and analysis package. We acknowledge use of the Legacy Archive for Microwave Background Data Analysis (LAMBDA). Support for LAMBDA is provided by the NASA Office of Space Science. This work was partially funded by ERC-2010-StG Grant 257080.

REFERENCES

Bennett, C. L., et al. 2011, ApJS, 192, 17

Bielewicz, P., & Banday, A. J. 2011, MNRAS, 412, 2104

Cornish, N., Spergel, D., & Starkman, G. 1998, Class. Quant. Grav., 15, 2657

Feeney, S. M., Johnson, M. C., Mortlock, D. J., & Peiris, H. V. 2010, arXiv:1012.3667

Fialkov, A., Itzhaki, N., & Kovetz, E. D. 2010, J. Cosmol. Astropart. Phys., JCAP02(2010)004

Gold, B., et al. 2011, ApJS, 192, 15

Górski, K. M., Hivon, E., Banday, A. J., Wandelt, B. D., Hansen, F. K., Reinecke, M., & Bartelman, M. 2005, ApJ, 622, 759

Gurzadyan, V. G., & Penrose, R. 2010, arXiv:1011.3706

Jarosik, N., et al. 2011, ApJS, 192, 14

Komatsu, E., et al. 2011, ApJS, 194, 18

Kovetz, E. D., Ben-David, A., & Itzhaki, N. 2010, ApJ, 724, 374

Liddle, A. R., & Lyth, D. H. 2000, in Cosmological Inflation and Large-Scale Structure, ed. A. R. Liddle & D. H. Lyth (Cambridge: Cambridge Univ. Press), 414

Moss, A., Scott, D., & Zibin, J. P. 2010, arXiv:1012.1305

Penrose, R. 2008, in On Space and Time, Causality, Quantum Theory and Cosmology, ed. S. Majid (Cambridge: Cambridge Univ. press), 141

Penrose, R. 2009, in Death and Anti-Death, Vol. 6: Thirty Years After Kurt Gödel (1906-1978), The Basic Ideas of Conformal Cyclic Cosmology, ed. C. Tandy (Stanford, Palo Alto, CA: Ria Univ. Press), 223, chap. 7

Penrose, R. 2010, Cycles of Time: An Extraordinary New View of the Universe (London: Bodley Head)